Superposition model for steady state visually evoked potentials

Jaiber Cardona*, Eduardo Caicedo**, Wilfredo Alfonso**, Ricardo Chavarriaga***, José del R. Millán***
* Universidad del Quindío/Facultad de Ingeniería, Armenia, Colombia
** Universidad del Valle/EIEE, Cali, Colombia
*** Chair on Non-Invasive Brain-Machine Interface (CNBI), Center for Neuroprosthetics,
Ecole Polytechnique Fédérale de Lausanne, Geneva, Switzerland

jaibercardona@uniquindio.edu.co, eduardo.caicedo@correounivalle.edu.co, wilfredo.alfonso@correounivalle.edu.co,
ricardo.chavarriaga@epfl.ch, jose.millan@epfl.ch

Abstract— **Steady State Visually Evoked Potentials (SSVEP) are signals produced in the occipital part of the brain when someone gaze a light flickering at a fixed frequency. These signals have been used for Brain Machine Interfacing (BMI), where one or more stimuli are presented and the system has to detect what is the stimulus the user is attending to. It has been proposed that the SSVEP signal is produced by superposition of Visually Evoked Potentials (VEP) but there is not a model that shows that. We propose a model for a SSVEP signal that is a superposition of the response due to the rising and falling edges of the stimulus and that can be calculated for different frequencies.**

We fixed the model for 4 subjects that gazed stimuli in the frequencies of 9Hz, 11Hz, 13Hz and 15Hz, and duty-cycles of 20%, 35%, 50%, 65%, and 80%. Since the phases of SSVEP signals are stable over the time, these were used to fix the model, without the amplitude; however, signals of scattered phases were discarded. The model parameters were found using the Oz electrode signals and a genetic algorithm.

The mean absolute error (MAE) between the measured phase and the obtained one was calculated for each subject (named S1, S2, S3, and S4). The model was fixed for the subjects in the fundamental frequencies, just two of them in the second harmonic, and one in the third harmonic. We obtained a maximum MAE for 3 subjects (S1, S2, and S4) in the fundamental frequencies at 0.30 rad and one of them (S2) with 0.21 rad in the second harmonic. The last one (S3) signals show poor results with a MAE between 0.46 rad and 1.79 rad by including fundamental frequencies, and second and third harmonics. The results show similarities among the different model parameters such that it suggests that a general model could be obtained.

I. Introduction

The Steady State Visually Evoked Potentials (SSVEP) signals are evoked when someone gaze a light flickers at a constant frequency. The SSVEP signals are used in Brain Machine Interfaces (BMI) in applications such as teleoperation control of an exoskeleton robot [1], wheelchair movement control [2], telepresence control of humanoid robot [3], speller system [4], among others.

The two major approaches to define the form of the stimuli in a SSVEP-based BMI are frequency modulation (f-VEP) and code modulation (c-VEP) [5]. In an f-VEP each stimulus flicker with rectangular signal, while in a c-VEP each stimulus flicker according to a binary code. A c-VEP scheme can yield higher communication rates and better accuracies [5] but the methodologies to define the binary code are still not well defined.

Variations in the duty-cycle of f-VEP scheme can generate different amplitudes and phases of SSVEP signals [7], but there is no clear understanding of such variations. In fact, the duty-cycle of a SSVEP stimulus is usually fixed at 50% without any consideration. However, it is possible that proper stimuli settings (i.e., a suitable duty-cycle) get more discriminant SSVEP responses.

Some works suggest that SSVEP signals are a superposition of Visual Evoked Potentials (VEP) [7] [8]. However, there is evidence of non-linear behavior in SSVEP signals [9]. Following the former assumption, we propose a model that represents SSVEP signals, as the superposition of the responses in rising and falling edges for each stimulus. The model is adjusted without taking into account the amplitude; -that can vary in the time-, focusing only on the phase between the stimulus and the SSVEP response, which is more stable [10].

Better understanding of the relation between the stimuli characteristics and the evoked response can help to improve SSVEP-based BMI in at least three forms: to identify subject-specific duty-cycles that generate more discriminant SSVEP signals, to generate new binary codes for c-VEP schemes that enhance SSVEP signals in the fundamental frequency or its harmonics, or to build new methods in SSVEP detection taking advantage of the SSVEP signal phase in addition to the amplitudes. As far as our knowledge, this is the first time that a model of this type has been proposed.

II. Methods

A. SSVEP Model

Assume that the SSVEP response, $f_s(t)$, in a f-VEP scheme with a period T_s in the stimulus is the addition of two signals:

$$f_s(t) = f_r(t) + f_a(t - t_a) \quad (1)$$

where $f_r(t)$ is the response due to the rising edges in the stimulus, $f_a(t)$ is the response due to the falling edges in the stimulus, and t_a is a value between 0 and T_s which is

the time when the falling edge is produced. Because of the first rising edge of the stimulus is taken as a reference of the time signal, there is not displacement in time for $f_r(t)$, and a rising edge is produced in $t=0$.

By applying Fourier transform to (1), we get

$$F_s(kw_s) = F_r(kw_s) + F_a(kw_s)e^{-jkw_s t_a} \quad (2)$$

where w_s is the frequency of the stimulus, k=1,2,3,… is the number of the harmonic, $F_s(w)$ is the Fourier transform of the SSVEP signal, and $F_r(w)$ and $F_a(w)$ are the Fourier transform of the rising and falling edge responses, respectively. The term kw_s is used to represent that the SSVEP signal is only present in the harmonics of the stimulus fundamental frequency.

The expression $w_s t_a$ can be rewritten as a function of the duty cycle d:

$$w_s t_a = 2\pi \frac{t_a}{T_s} = 2\pi d \quad (3)$$

We assume that the Fourier transform of the rising and falling edge responses have constant coefficients for each harmonic:

$$F_r(kw_s) = A_{rk}e^{-jw_{rk}}$$
$$F_a(kw_s) = A_{ak}e^{-jw_{ak}} \quad (4)$$

where A_{rk} and A_{ak} are positive scalars, and w_{rk} and w_{ak} are angles for the k-harmonic.

By replacing (3) and (4) in (2), we obtain:

$$F_s(kw_s) = A_{rk}e^{-jw_{rk}} + A_{ak}e^{-jw_{ak}}e^{-j2\pi kd} \quad (5)$$

In addition, we define the terms

$$A_k = A_{rk} + A_{ak}$$
$$R_k = A_{rk}/(A_{rk} + A_{ak}) \quad (6)$$

to rewrite (5)

$$F_s(kw_s) = A_k H(k) \quad (7)$$

where

$$H(k) = (R_k e^{jw_{rk}} + (1-R_k)e^{jw_{ak}-j2\pi kd}) \quad (8)$$

being R_k a scalar between 0 and 1 at the harmonic k.

The duty-cycle, d, in $H(k)$ defines the angle that the falling edge response is rotated for getting the final value of the Fourier coefficients. This condition is depicted in Fig. 1 for the fundamental frequency (k=1).

The $H(k)$ amplitude has a minimum when the rising and rotated falling edge response coefficients have opposite directions, and its value is the absolute value of $(1-2R_k)$. Notice that when R_k is close to 0.5 the duty-cycle can lead this amplitude near zero. Otherwise, the $H(k)$ amplitude has a maximum when the rising and rotated falling edge response coefficients have the same direction, and its value is 1; here, the term R_k indicates the percentage of contribution of the rising edge response coefficients in $H(k)$.

Eq. (8) can be rewritten as

$$H(k) = e^{jw_{rk}}(R_k + (1-R_k)e^{j(w_{ak}-w_{rk})-j2\pi kd}) \quad (9)$$

where $H(k)$ amplitude depends on (w_{ak}-w_{rk}), d, k, and R_k.

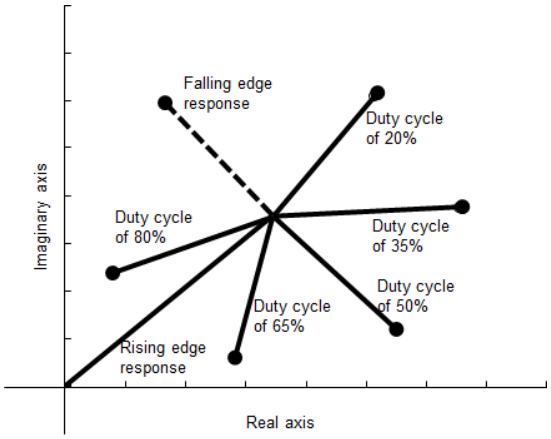

Figure 1. Final coefficients are the addition of rising and falling edge responses

The amplitude and phase variations for the fundamental frequency ($k=1$) of $H(k)$ as a function of the duty-cycle are depicted in Fig. 2 and Fig. 3 for $(w_{a1} - w_{r1}) = \pi/2$.

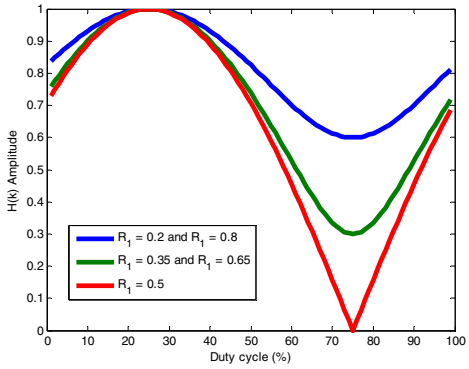

Figure 2. $H(k)$ amplitude variation for the fundamental frequency as a function of duty cycle at $(w_{a1} - w_{r1}) = \pi/2$

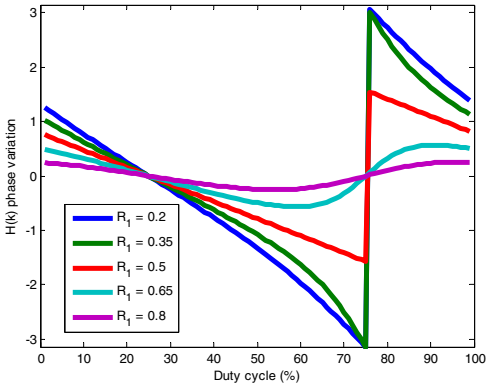

Figure 3. $H(k)$ phase variation for the fundamental frequency as a function of duty cycle at $(w_{a1} - w_{r1}) = \pi/2$.

R_1 defines the minimum of $H(k)$ amplitude and how the phases, from different duty-cycles, are scattered.

The difference (w_{a1}-w_{r1}) defines the position of the two graphs. When (w_{a1}-w_{r1}) increases (decreases) the graphs are placed to the right (left). This condition is depicted in Fig. 4 and Fig. 5 for $R_1=0.4$.

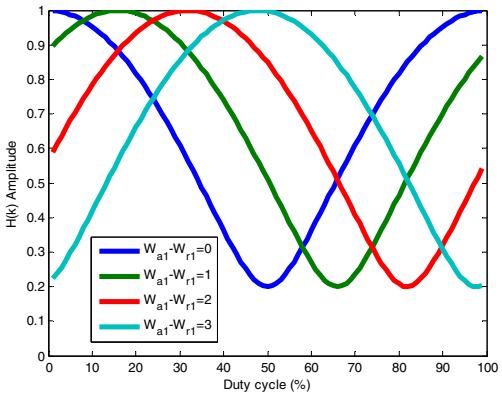

Figure 4. *H(k)* amplitude variation for the fundamental frequency as a function of duty cycle at R_1=*0.4*.

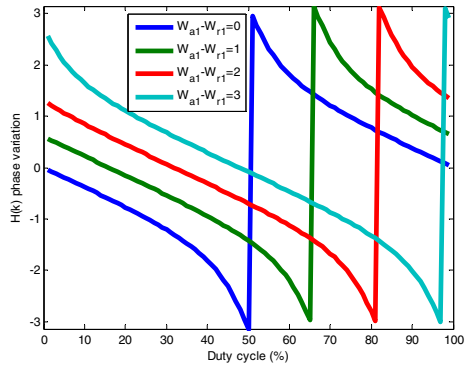

Figure 5. *H(k)* phase variation for the fundamental frequency as a function of duty cycle for R_1=*0.4*.

The phase and amplitude variations for the second harmonic have the same form as it is shown in Fig. 2 and Fig. 3, but it is repeated twice: one for a duty-cycle between 0% and 50%, and other for a duty-cycle between 50% and 100%. When the duty-cycle changes between 0% and 100%, the term $e^{-j2\pi kd}$ (see, Eq 5) is turned *k*-times around the imaginary plane.

The final *H(k)* phase and amplitude varies accordingly to the duty-cycle value, and therefore the final SSVEP amplitude signal would also change. Since the *H(k)* amplitude varies from 0 to 1, then the final amplitude of the SSVEP signal can be strongly modified by the duty-cycle.

The optimal duty-cycle (ODC) –i.e., the one that evokes stronger responses- would be the one that put the responses to the two signals (i.e. rising and falling edge) in the same direction. Conversely, the worst would be the one that put the two signals in opposite directions.

The SSVEP amplitude signal can variate for different reasons. Here, we assume that these changes affect both rising and falling edge responses in the same manner, so we define R_k as a constant. Furthermore, the phase of the stimulus response is constant [10], we will define w_{ak} and w_{rk} as constants. Therefore, the SSVEP spectral content would be mainly modulated by the A_k amplitude and the duty-cycle, as it is shown in (7).

B. *Experimental protocol*

To validate the model, we tested it on 4 subjects (1 female; ages of 20, 40, 62 and 73) without known mental illness and without mental illness in their family history.

Subjects were asked to gaze at a LED display flickering at different frequencies and duty-cycles. The frequencies were 9Hz, 11Hz, 13Hz, and 15Hz; and the duty-cycles were 20%, 35%, 50%, 65% and 80%. Stimulation on a given frequency and duty-cycle lasted for 6 seconds, interleaved by no stimulation resting periods of 4s. Each subject performed 5 runs comprising all conditions (frequencies and duty-cycles), with 2 min pauses between runs. Every run lasted 200s. The frequency and duty-cycle pairs were organized in a pseudorandom order that was applied in the runs for all subjects. As it is customary for these experiments, subjects were instructed to avoid blinking during the stimulation periods and to refrain from moving during all the procedure.

We recorded EEG signals using an eighth channels OpenBCI system with a sampling frequency at 250Hz. Electrodes were located in PO3, PO4, PO7, PO8, POz, Oz, O1 and O2 of the 10/10 system [11], the ground and reference were placed in the left and right mastoid, respectively. To measure the phase difference between the visual stimulus and the EEG response, we recorded the LED status as a hardware trigger in the OpenBCI. Just Oz was used for the analysis.

C. *Parameter selection*

The A_k variation is unknown for our model but it does not modify the phase since it is a positive scalar, thus, it is possible to use the phase to get the *H(k)* parameters.

For every combination of frequency and duty-cycle, the Fourier transform coefficients were calculated in windows of 5s over the frequencies of interest. The first window started at the same moment that stimulation (frequency and duty-cycle) condition appeared and it was displaced in 4ms intervals until it arrived to 1s, to cover the 6s of stimulation. Thereby, the amount of Fourier transform coefficients were 251 for every pair frequency-duty-cycle in one run, i.e., 1255 for the five runs.

The data of every five seconds windows were forced to start at the same time of a rising edge of the stimulus to have the same reference in the phase.

We used the Component Synchrony Measure (CSM) [12] to estimate the synchrony of phase among the 251 values of the Fourier transform coefficients during the windows of five second,

$$CSM = \left(\frac{1}{n}\sum_{i=1}^{n}\cos w_i\right)^2 + \left(\frac{1}{n}\sum_{i=1}^{n}\sin w_i\right)^2 \qquad (10)$$

where w_i is the phase and n is the amount of Fourier transform coefficients (n=251 for our protocol). The value of CSM $\in$ [0, 1] is close to 0 if the phases are scattered but this value increases as the phases get closer.

Conditions (i.e., combination frequency and duty-cycle in one run) with CSM<0.75 are discarded from further analysis, since this shows no relation between the stimulation and the SSVEP response.

To build the model, we compute the average phase of the 251 Fourier transform coefficients of each combination frequency and duty-cycle in one run. Only

those conditions that had at least 4 runs with CMS≥0.75, in at least 4 duty-cycles, were taken into account. Therefore, for every selected frequency we had a minimum of 16 and a maximum of 25 pairs of duty-cycle and phase to fit the model. We use the last run to validity the model, which corresponds a percentage between 20% and 25% of the data.

The model parameters were tuned for every frequency and subject by minimizing the performance index,

$$J = \frac{1}{P}\sum_{p=1}^{P}\left|w_p - \hat{w}_p\right| \qquad (11)$$

where J is the mean absolute error (MAE) value, w_p is the measured phase, $\hat{w}_p$ is the obtained phase of the model in (8), and P is the number of pairs duty-cycles and phases used to fit the model.

To minimize the performance index we used a genetic algorithm [13] that was configured with 3 characteristics in each candidate solution: w_r, w_a, and R. The population size was set to 20 for all the generations with initials conditions of random values between $-\pi$ and π for w_r and w_a, and between 0 and 1 for R. The genetic algorithm runs for 1000 generations. The candidate solutions in one generation were selected by applying 3 genetics operators in the previous generation: elite, mutation and inheritance. In every generation the elite, mutation, and inheritance operators were applied 2, 6 and 12 times correspondingly.

In the elite operator the 2 candidate solutions with the best performance indexes are selected, in the mutation operator one random candidate solution is selected and one of its characteristics is modified by adding a random number between -0.1 and 0.1, and in the inheritance operator two random candidate solutions are selected and their characteristics are averaged.

These three parameters allow us to calculate the ODC which is the duty cycle value that yields the same direction in the rising edge and falling edge responses.

III. RESULTS

The values of w_{rk}, w_{ak}, and R_k parameters were obtained for the data that fulfill the conditions explained in section II.C. The calculations were made for the fundamental frequency and the second and third harmonic. There were not data that fulfill the condition in the fourth harmonic.

Only 9 subject-frequency pairs satisfied the conditions in section II.C for the fundamental frequency, 4 for the second harmonic, and 1 for the third harmonic. It is expected that this number of pairs decreases when the harmonic number increases. The rising and falling edges appear *1/k* times for period in average for the *k*-harmonic frequency. So, the signal is weaker when *k* is increasing.

Fundamental frequency

The list of subject-frequency pairs that satisfied the condition to fix the model at the fundamental frequency is shown in Table I. It also reports the number of duty-cycle and frequency pairs used to fix the model, the MAE obtained after tuning the model, and the validation MAE. It is shown that with the exception of S3, the model yields MAEs less than 0.30 rad.

TABLE I.
DATA FOR MODEL FIX IN THE FUNDAMENTAL FREQUENCY

Sub	Freq	Num of pairs	MAE	Val. MAE
S1	13Hz	19	0.30 rad	0.13 rad
S1	15 Hz	19	0.23 rad	0.32 rad
S2	9 Hz	24	0.18 rad	0.20 rad
S2	11 Hz	24	0.18 rad	0.14 rad
S2	13 Hz	16	0.17 rad	0.27 rad
S3	9 Hz	22	0.46 rad	1.19 rad
S3	13 Hz	24	0.46 rad	0.95 rad
S4	13 Hz	17	0.12 rad	0.24 rad
S4	15Hz	17	0.07 rad	0.24 rad

To better understand the meaning of MAE in the phase, the differences between the measured and the estimated phases, in one subject at 15Hz for the first run, are shown in Fig. 6, where the maximum difference between the measured and estimated phases was 0.26 rad for a duty-cycle of 35%.

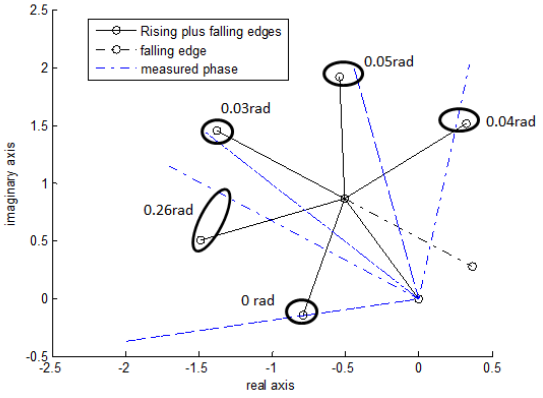

Figure 6. Differences of measured and obtained phases for a subject in 15Hz

The estimated phases, w_{r1} (circles) and w_{a1} (diamonds), are depicted in Fig. 7, where blue, red, black and green markers are corresponding to S1, S2, S3 y S4, respectively. We can see that these phases are located in different regions of the graph; for sake of clarity we added lines to delineate these regions. The region in the center belongs to the phases of falling edge responses (w_{a1}), and the regions in the extremes belong to the phases of rising edge responses (w_{r1}). Only the phase of the falling edge response for S3 in 9Hz appears in the wrong region. Notice that this is the combination that showed the highest error (cf. Table I).

These two regions suggest that the behavior of the SSVEP responses is similar in phase and amplitude among the subjects, and a general model could be obtained; however, more experiments are need to fully verify this finding.

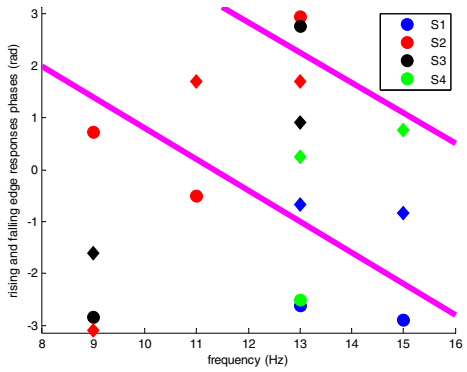

Figure 7. Estimated values of w_{r1} (circles) and w_{a1} (diamonds)

The estimated value of R_1 for different frequencies is depicted in Fig. 8. This value changes between 40% and 70% suggesting that the contribution of rising and falling edge responses to ODC are approximately equal, and both have strong influence in the amplitude and phase of *H(k)* and, hence, in the final SSVEP signal. Additionally, a value of R close to 50% means that the SSVEP signal will be modulated by the direction (phase) of the responses to the falling and rising edge, which, as shown above depends strongly on the duty-cycle (see Fig 1).

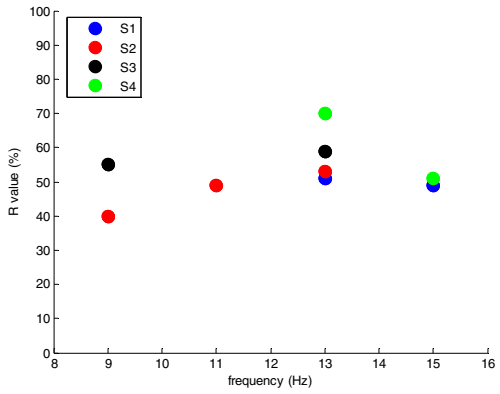

Figure 8. R_1 value as a function of the frequency

The calculated ODC for the model under conditions in Table I is depicted in Fig. 9. Some ODC values are far from a duty-cycle of 50%, it would suggest that a 50% duty-cycle yields less amplitude than others duty-cycles.

Second harmonic

The list of subject-frequency pairs that satisfied the condition to fix the model for the second harmonic are shown in Table II, It also reports the number of pairs duty-cycle and frequency used for fix the model, the MAE used to tune the model, and the validation MAE.

For S2, the MAE is similar to theses that were obtained in the fundamental frequency, but it was only obtained at 15 Hz where a model in fundamental frequency was not calculated. The low value of the MAE for S2 indicates that the model expresses the behavior of the phase for the second harmonic.

In S3, the MAEs were similar to theses in the fundamental frequency. Taking into account the fundamental frequency and second harmonic, the maximum MAE for S3 was 1.19 rad that corresponds to a 19% of the imaginary plane. Despite this value looks high, it marks a zone in the imaginary plane where the final Fourier transform coefficients should be.

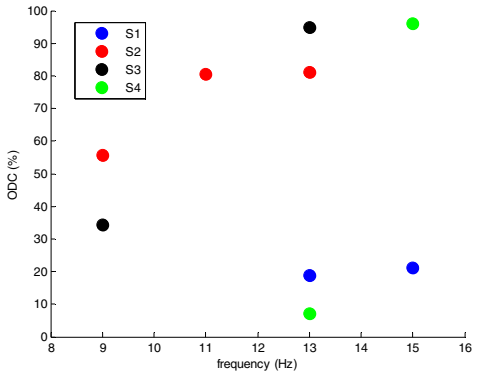

Figure 9. ODC values for fundamental frequency.

TABLE II.
DATA FOR MODEL FIX IN THE SECOND HARMONIC

Sub	Freq	Num of pairs	MAE	Val. MAE
S2	30 Hz	19	0.17 rad	0.21 rad
S3	22 Hz	18	0.62 rad	0.45 rad
S3	26 Hz	22	0.55 rad	0.48 rad
S3	30 Hz	18	0.51 rad	1.17 rad

The estimated phases, w_{r2} (circles) and w_{a2} (diamonds), are depicted in Fig. 10. Similar to fundamental frequency, there are two regions that contain the phases due to rising and falling edge responses. For sake of clarity, we added a line to delineate these regions.

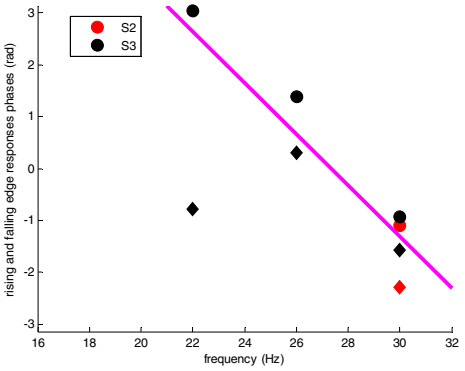

Figure 10. Estimated values of w_{r2} (circles) and w_{a2} (diamonds)

The value estimated of R_2 for different frequencies is depicted in Fig. 11. This value changes between 50% and 70%. This suggests that the contribution of rising and falling edge responses in the ODC for the second harmonic are similar, and both have strong influence in the final amplitude and phase of *H(k)*. The values of R_2 are close to 50% as the fundamental frequency case.

The calculated ODC for the model under conditions in Table II is depicted in Fig. 12. Some ODC values are far from a duty-cycle of 25% -Equivalent to 50% in fundamental frequency- it would suggest that a 50% duty-

cycle yields less amplitude than others duty-cycles in the second harmonic.

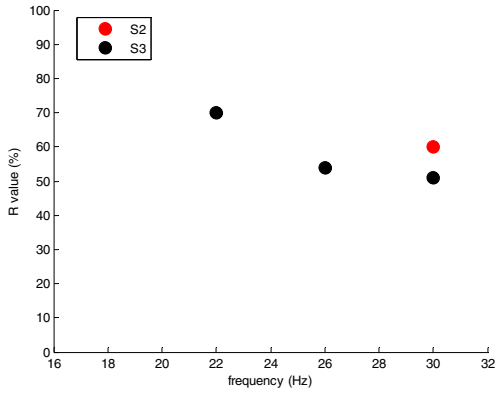

Figure 11. R_2 value as a function of the frequency.

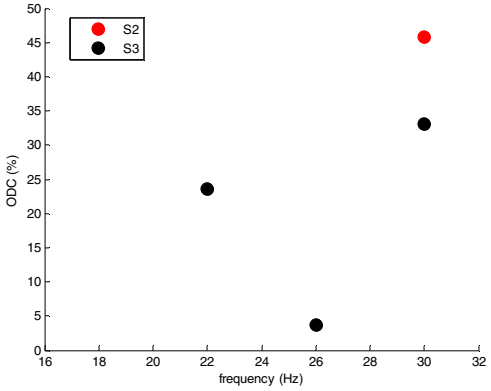

Figure 12. ODC values for second harmonic

Third harmonic

In the third harmonic only S3 fulfilled the conditions for fix the model at 27 Hz (i.e., 3 times 9 Hz) with 17 duty-cycle and phase pairs. The MAE was 0.8183 and the validation MAE was 1.7935. The MAEs are pretty large and hence, they do not show relation between the model and the data of the third harmonic; other subject and frequency pairs did not fulfill the conditions of section II.C to fix the model. Notice that the pair S3 and 9Hz had a high MAE when its data were used to fix the model in the first harmonic and it did not appear in the second harmonic.

IV. Conclusions

We present a first approach to model the superposition in SSVEP signal that can be fixed for different frequencies of one subject. The MAEs found in 3 of 4 subjects were low which indicate that the model can predict the phase in a SSVEP signal evoked by a stimulus in the f-VEP scheme.

The model is based in the superposition of rising and falling edge responses and it worked in the fundamental frequency and the second harmonic. In addition, it shows the phase and amplitude behavior in higher harmonics.

The model predicts the phase in different duty-cycles, whereby, it could be the foundation for new methodologies of SSVEP detection based on the phase and it could be extended to stimulus in the c-VEP scheme; however, other experiments should develop to verify its functionality.

References

[1] Qiu S., Li Z., He W., Zhang L., Yang C., Su C. Teleoperation control of an exoskeleton robot using brain machine interface and visual compressive sensing. IEEE Transactions on Fuzzy Systems. Vol. PP, no. 99, 2016. IEEE Early Access Articles.

[2] Li Y., Pan J., Wang F., Yu Z. A hybrid BCI system combining P300 and SSVEP and its application to wheelchair control. IEEE Transactions on Biomedical Engineering. Vol 60, no 11, pp. 3156 – 3166, 2013.

[3] Zhao J., Li W., Mao X., Hu H., Niu L., Chen G. Behavior-based SSVEP hierarchical architecture for telepresence control of humanoid robot to achieve full body movement. IEEE Transactions on Cognitive and Developmental Systems. Vol. PP, no 99, 2016. IEEE Early Access Articles.

[4] Akce A., Norton J., Bretl T. An SSVEP-based brain–computer interface for text spelling with adaptive queries that maximize information gain rates. IEEE Transactions on Neural Systems and Rehabilitation Engineering. Vol. 23, no. 5, pp. 857 – 866. 2015.

[5] G. Bin, X. Gao, Y. Wang, B. Hong, and S. Gao, "Vep-based braincomputer interfaces: time, frequency, and code modulations [research frontier]," Computational Intelligence Magazine, IEEE, vol. 4, no. 4, pp. 22–26, 2009

[6] Huang G., Yao L., Zhang D., Zhu X., Effect of duty-cycle in different frequency domains on SSVEP based BCI: A preliminary study. Engineering in Medicine and Biology Society (EMBC), 2012 Annual International Conference of the IEEE

[7] Gaume, A; Vialatte, F.; Dreyfus, G., "Detection of steady-state visual evoked potentials using simulated trains of transient evoked potentials," Faible Tension Faible Consommation (FTFC), 2014 IEEE , vol., no., pp.1,4, 4-6 May 2014

[8] Bohorquez, J. Lozano, S. ; Kao, A. ; Toft-Nielsen, J. ; Ozdamar, O. Deconvolution and Modeling of Overlapping Visual Evoked Potentials. Biomedical Engineering Conference (SBEC), 2013 29th Southern.

[9] Notbohm, Annika; Kurths, Jürgen; Herrmann, Christoph S. Modification of brain oscillations via rhythmic light stimulation provides evidence for entrainment but not for superposition of event-related responses. Frontiers in Human Neuroscience. Volume 10, Issue FEB2016, 3 February 2016, Article number 10.

[10] Burkitta, Guy R.; Silbersteina, Richard B.; Caduschb, Peter J.; Wood, Andrew W. Steady-state visual evoked potentials and travelling waves. Clinical Neurophysiology, Volume 111, Issue 2, 1 February 2000.

[11] J. Valer, D. Tsuzuki, and D. Ippeita. "10/20, 10/10, and 10/5 systems revisited: Their validity as relative head-surface-based positioning systems," in NeuroImage Vol. 34 ,2007, pp. 1600–1611.

[12] Ross Cunnington, Kian B. Ng, and Bradley, Andrew P. Enhancing the classification accuracy of Steady-State Visual Evoked Potential-based Brain-Computer Interface using Component Synchrony Measure. WCCI 2012 IEEE World Congress on Computational Intelligence. - Brisbane, Australia. June, 10-15, 2012

[13] Zbigniew Michalewicz, "Genetic algorithms + data structures = evolution programs". New York, Springer-verlag. 1999.